JACS
JOURNAL OF THE AMERICAN CHEMICAL SOCIETY

Communication

pubs.acs.org/JACS

Platonic Hexahedron Composed of Six Organic Faces with an Inscribed Au Cluster

Masanori Sakamoto,[†,‡,¶] Daisuke Tanaka,[†,‡] Hironori Tsunoyama,[§] Tatsuya Tsukuda,[§] Yoshihiro Minagawa,[‡,∥] Yutaka Majima,[‡,∥,⊥] and Toshiharu Teranishi*[,†,‡,#]

[†]Faculty of Pure and Applied Sciences, University of Tsukuba, Tsukuba 305-8571, Japan

[‡]CREST, Japan Science and Technology Agency (JST), Yokohama 226-8503, Japan

[¶]PRESTO, JST, Tsukuba 305-8571, Japan

[§]Section of Catalytic Assemblies, Catalysis Research Center, Hokkaido University, Sapporo 001-0021, Japan

[∥]Materials and Structures Laboratory, Tokyo Institute of Technology, Yokohama 226-8503, Japan

[⊥]Department of Printed Electronics Engineering, Sunchon National University, Sunchon 540-742, Korea

[#]Institute for Chemical Research, Kyoto University, Uji 611-0011, Japan

Supporting Information

ABSTRACT: The structures of nanomaterials determine their individual properties and the suprastructures they can form. Introducing anisotropic shapes and/or interaction sites to isotropic nanoparticles has been proposed to extend the functionality and possible suprastructure motifs. Because of symmetric anisotropy, Platonic solids with regular polygon faces are one of the most promising nanoscale structures. Introduction of Platonic solid anisotropy to isotropic nanomaterials would expand the functionality and range of possible suprastructure motifs. Here, we demonstrate a novel strategy to obtain nano-Platonic solids through the face coordination of square porphyrins on an inscribed Au sphere with adequate size. The face coordination of the multidentate porphyrin derivatives, with four acetylthio groups facing the same direction, on the Au cluster encased the Au cluster in a Platonic hexahedron with six porphyrin faces. Transmission electron microscopy, mass spectrometry, elemental analysis, and scanning tunnelling microscopy were used to confirm the formation of the nano-Platonic hexahedron.

The structure of a nanomaterial is an important parameter that determines its individual characteristics and the suprastructures that it can form through assembly.[1] Because of symmetric anisotropy, Platonic solids are one of the most promising nanoscale structures. A Platonic solid is a convex polyhedron with congruent regular polygon faces and identical polyhedral angles. Regular tetrahedron, hexahedron, octahedron, dodecahedron, and icosahedron are known to be Platonic solids. Various nanoscale Platonic solids, from nanoparticles to molecular cages, have attracted considerable attention because of the potential to control their nanostructures and the functionalities of both individual and assembled structures.[2]

An inscribed sphere inside a Platonic solid is tangent to the center of each face. Deliberate adhesion of the face of regular polygon on an isotropic sphere results in the formation of the anisotropic Platonic solid. It should be emphasized that anisotropy in shape and interaction is a key to regulation of the possible arrangement of a suprastructure. Introducing anisotropic shapes and/or interaction sites to isotropic nanomaterials is essential for expansion of the functionality and range of possible suprastructure motifs. Isotropic building blocks with specific surface modifications, such as DNA linkers and attractive patches, have been proposed for controllable formation of suprastructures.[3] Moreover, Stellacci et al. demonstrated that a metal nanoparticle with two coordination sites at polar positions can be linked to form nanoparticle chains.[4] However, these pathways are limited for assembly of isotropic nanomaterials, and a novel strategy for this needs to be developed. The encasement of an isotropic nanoparticle in a Platonic solid is an alternative solution for design of nanomaterials with specific and anisotropic surface functionalities. This method could be extended to the controllable formation of a nanoparticle suprastructure. This will allow development of novel materials with new collective phenomena. While this concept is simple in theory, the assembly of regular polygonal molecules on a metal sphere is extremely difficult in practice and has not been successful.

Here, we detail the construction of a Platonic solid from square porphyrins and a Au sphere. A regular hexahedron was formed by face coordination of square porphyrins on a suitable metal cluster, instead of attaching the sides of the porphyrins to each other (Figure 1). This approach relies on the face coordination of porphyrins on a Au cluster with a similar size to the porphyrin. For this purpose, we synthesized the following multidentate macrocyclic porphyrin thioester derivatives: tetrakis-5α,10α,15α,20α-(2-acetylthiomethylphenyl) porphyrin (SC_1P) and tetrakis-5α,10α,15α,20α-(2-acetylthioethylphenyl) porphyrin (SC_2P) (Figure 1a).[5] The SC_nP (n = 1 or 2) ligands contain four acetylthio groups that face the same direction and offer a quadridentate coordination site that cooperates with the π-system of the macrocycle to bind Au clusters in a face-coordination fashion (Figure 1b). The face coordination of

Received: October 13, 2011
Published: December 21, 2011

   dx.doi.org/10.1021/ja209634g | J. Am. Chem.Soc. 2012, 134, 816–819

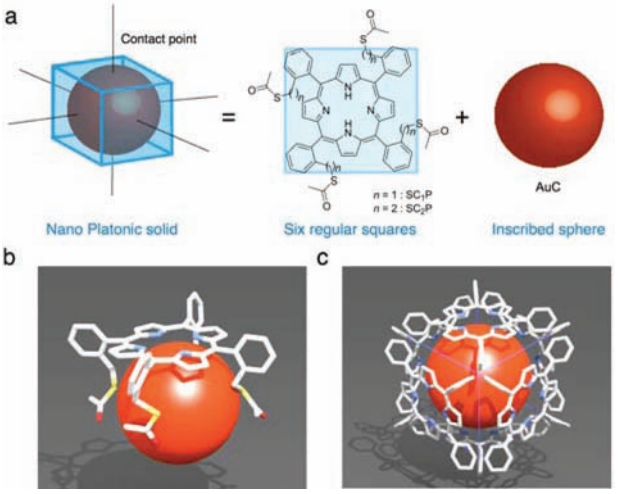

Figure 1. (a) Strategy for assembling the platonic solid from porphyrins and a Au cluster. Chemical structures of SC_nP are also shown. (b) Schematic illustration of the coordination fashion of SC_1P on the Au cluster. Hydrogen atoms are omitted for clarity. (c) Schematic illustration of the Platonic hexahedron constructed with six porphyrin faces and an inscribed Au sphere. Only the tetraphenylporphyrin moieties are shown for clarity.

SC_nP on the Au cluster results in the formation of the regular hexahedron with congruent porphyrin faces, as shown in Figure 1c.

The Au clusters coordinated by the SC_nP (SC_nP–AuCs) were synthesized by reduction of Au(III) ions in CH_2Cl_2/CH_3OH at 200 K in the presence of SC_nP (see the Supporting Information (SI) for detail). The obtained SC_nP–AuCs were isolated by gel permeation chromatography (GPC). Figure 2a

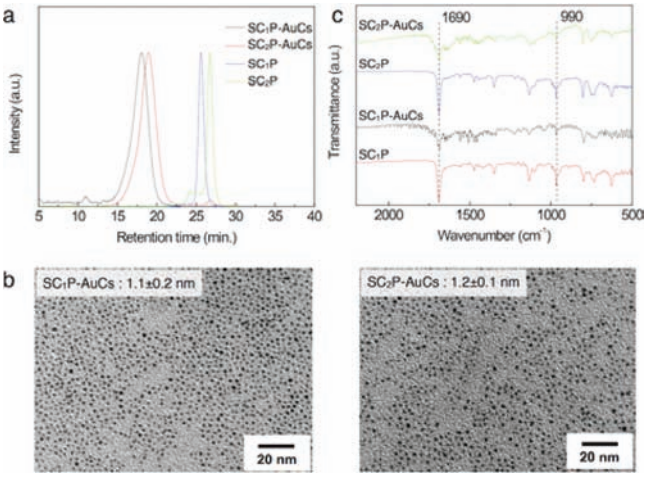

Figure 2. (a) Typical chromatograms of SC_nP–AuCs and SC_nP. (b) TEM images of SC_nP–AuCs. (c) FT-IR spectra of SC_nP and SC_nP–AuCs.

shows typical GPC chromatograms of the SC_nP–AuCs. Each SC_nP–AuC showed only one peak with a highly reproducible retention time. The peak shapes of SC_nP–AuCs in the GPC chromatograms had Gaussian distributions, which indicates that the obtained SC_nP–AuCs consist of single components. The retention time of the SC_2P–AuCs was slightly less than that of the SC_1P–AuCs, which suggests that the SC_2P–AuCs are only slightly larger in volume than the SC_1P–AuCs because of the larger ligand size. Transmission electron microscope images of the SC_nP–AuCs are shown in Figure 2b. Highly monodisperse clusters with sizes of 1.1 ± 0.2 and 1.2 ± 0.1 nm were observed for the SC_1P– and SC_2P–AuCs, respectively. It is noteworthy that the formation of the monodisperse Au clusters was only observed when *α,α,α,α*-isomers were employed as protecting ligands. Using other conformational isomers resulted in the formation of aggregates of polydisperse Au clusters, which were derived from cross-linking of the Au clusters by the ligands with four acetylthio groups facing in the separate direction. The face-coordination of *α,α,α,α*-SC_nP on the Au cluster strongly protects the core and suppresses this cross-linking.

Fourier transform infrared spectroscopy provided further evidence for face coordination of SC_nP on the Au clusters. Figure 2c shows the Fourier transform infrared spectra of SC_nP and the SC_nP-AuCs. For the SC_nP ligand, several strong peaks were observed at 1690 and 990 cm^{-1}, which can be attributed to the carbonyl stretching vibration of the acetylthio group and pyrrole ring breathing motion, respectively.[6] Similar peaks were also observed for the SC_nP–AuCs, which indicates that the SC_nP ligand attaches to the Au clusters. Because the carbonyl stretching vibration was observed for the SC_nP–AuCs, it can be concluded that the acetyl groups were not dissociated during cluster formation. When the Au clusters were synthesized in the similar manner using benzylthioacetate (SC_1) as a protecting ligand, tetraoctylammonium-protected Au clusters were formed instead of SC_1-protected Au clusters; tetraoctylammonium was used to dissolve Au(III) ions in the organic phase (see SI). This result suggests that the acetylthio group is not able to bind to the Au surface as strongly as thiols or amines. Use of the quadridentate acetylthio group of SC_nP can overcome this and stably bond to the Au surface.

The absorption spectra of SC_nP and SC_nP–AuCs provided insights into the coordination fashion of SC_nP. As shown in Figure 3, the Soret bands of SC_nP on the Au clusters were

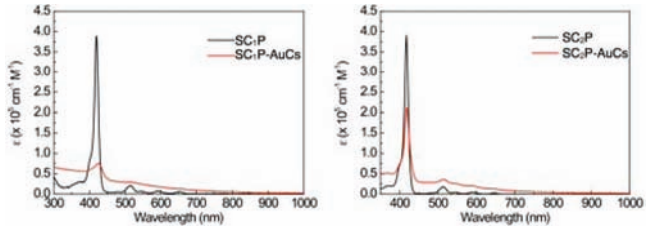

Figure 3. UV–vis-NIR spectra for SC_nP and SC_nP–AuCs in DMF. The extinction coefficients of SC_nP on SC_nP–AuCs were estimated from inductively coupled plasma atomic emission spectroscopy data.

broad, and the peak position for SC_1P was red-shifted compared to the free ligand. Furthermore, on coordination to the Au clusters, the extinction coefficients of SC_1P and SC_2P were reduced up to 9% (from 3.9×10^5 to 3.5×10^4 cm^{-1} M^{-1}) and 36% (from 3.9×10^5 to 1.5×10^5 cm^{-1} M^{-1}), respectively. From X-ray crystallography, the distance between the porphyrin ring and sulfur atoms was determined to be 3.45 and 4.85 Å for SC_1P and SC_2P, respectively (see SI). This indicates that the spectral shift and the reduction of the extinction coefficient depend on the distance between the porphyrin ring and the Au cluster. Similar spectral changes were observed for SC_1P-coordinated Au nanoparticles (approximately 10 nm in size) in an earlier study,[5] and the reason for this is currently under investigation. Possible explanations

dx.doi.org/10.1021/ja209634g | J. Am. Chem.Soc. 2012, 134, 816–819

for this change are (i) exciton coupling between the porphyrin moieties[7] and/or (ii) electronic interaction between the π-system of the porphyrin and the Au clusters. Although the suggested spatial arrangement of the porphyrins (i.e., hexahedron) indicates the existence of the excitonic interaction, the phenomena would not strongly depend on the distance between the porphyrin ring and the Au cluster. Thus, we consider that both phenomena work together and lead to the dramatic spectral changes. To construct the Platonic hexahedron, the center of each face should contact the inscribed sphere. The interaction between the porphyrin and the Au cluster is favorable for contact of the Au cluster with the porphyrin ring and leads to formation of a Platonic hexahedron.

We confirmed the chemical compositions of the SC_nP-AuCs by matrix-assisted laser desorption/ionization time-of-flight (MALDI TOF) mass spectrometry. Figure 4a shows the

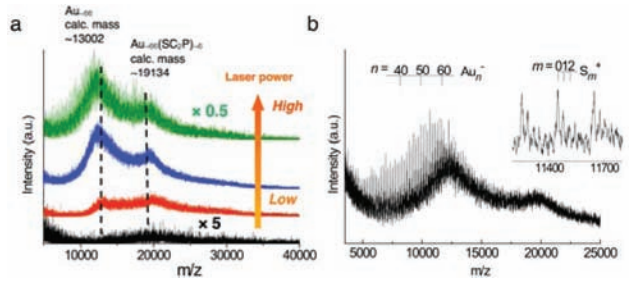

Figure 4. (a) MALDI-TOF mass spectra of SC_2P–AuCs at various laser powers. (b) MALDI-TOF mass spectra of SC_2P–AuCs at high laser power. Regular progressions of the mass spectra, which correspond to Au and sulfur atoms, were observed. The inset shows the expanded image of progressions of Au_n^- and $Au_nS_m^-$ ($m \geq 1$).

negative-ion MALDI TOF mass spectra of the SC_2P–AuCs recorded at various laser powers. At a minimum laser power, a broad (unresolved) peak was observed at approximately 19 kDa. A new peak appeared at approximately 13 kDa at a higher laser power, and its relative intensity to that of the 19 kDa peak increased with increasing laser power. These results indicate that the peaks at approximately 19 and 13 kDa can be assigned to the parent SC_2P–AuCs and their fragments, respectively. Since the mass difference between the two peaks (approximately 6 kDa) corresponds to the molecular weight of six SC_2P ligands (6132 Da), the fragment peak at 13 kDa could be assigned to the Au core composed of 66 ± 5 Au atoms. The mass spectral analysis suggests that the composition of SC_2P–AuCs is $Au_{\sim 66}(SC_2P)_{\sim 6}$, which is in agreement with that estimated from transmission electron microscopy and elemental analysis. For the SC_1P–AuCs, the mass peak for the Au core was observed at approximately 13 kDa at a higher laser power, whereas the mass peak assigned to the parent SC_1P–AuCs was not observed even at a lower laser power. Stronger interaction of the Au core with SC_1P than with SC_2P, suggested by the absorption spectra, may be responsible for this phenomenon, although this needs to be clarified. The number of Au atoms for the SC_1P–AuCs was estimated to be 65 ± 10. These numbers of Au atoms constructing the AuCs are different from the magic numbers that are known to thiol-protected or gas phase AuCs, suggesting that the SC_nP–AuCs are formed through the kinetic stabilization by specific SC_nP.

When the laser power was increased further, the progression of Au_n^- became more prominent in the MALDI TOF mass spectra of the SC_2P–AuCs (Figure 4b). Interestingly, the intensity of $Au_nS_m^-$ ($m \geq 1$) was much weaker than that of Au_n^- (see Figure 4b, inset). This feature is in sharp contrast to the laser desorption/ionization mass spectra of thiol-protected AuCs[8] but similar to those of polyvinylpyrrolidone-stabilized AuCs.[9] This result indicates that the Au–S bonds in the SC_2P–AuCs are much weaker than those in the thiol-protected Au clusters. The Au cores of the SC_nP–AuCs are stabilized by multiple weak interactions, which is similar to the Au clusters protected by polyvinylpyrrolidone.

To evaluate the SC_nP–AuCs as a whole, we attempted to determine the number of SC_nP on a single Au cluster using inductively coupled plasma atomic emission spectroscopy. The Au to sulfur atom amount-of-substance ratios were 74:26 and 73:27 for SC_1P– and SC_2P–AuCs, respectively, which indicates that 6 ± 1 SC_nP was attached on a single Au cluster. Since the GPC chromatograms indicated that the SC_1P–AuC and SC_2P–AuC had similar volumes, both clusters would show similar geometry with the same number of porphyrins. The most thermodynamically stable structure should have the lowest surface energy by complete coverage of the Au cluster surface. A hexahedron of six SC_nP ligands is likely to completely cover the Au cluster surface.

The scanning tunnelling microscopy (STM) provided further information on the structure of SC_nP–Au. The STM images of the SC_1P–AuCs are shown in Figure 5a.[10] Generally, the tip

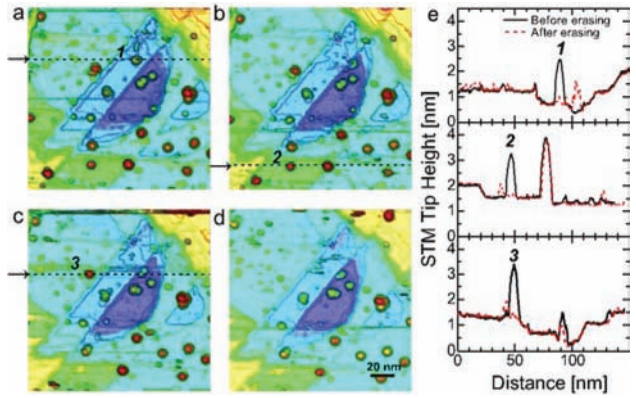

Figure 5. (a) A three-dimensional STM image of SC_1P–AuCs adsorbed on the Au(111)/mica surface at room temperature. The scanning area was 85 × 85 nm^2. The STM image is analyzed using WSxM.[13] (b–d) Three-dimensional STM images of SC_1P–AuCs adsorbed on the Au(111) surface after erasing manipulation of nanoclusters 1, 2, and 3 in (a). (e) The height profiles before (black line) and after erasing (red line). The erasing procedure was conducted as follows: the STM tip was positioned on the target SC_1P–AuC numbered in (a–c); a sample bias voltage of 3 V was applied to the substrate with a set point current of 50 pA for about 1 min; and the sample bias was decreased to 1.5 V and the STM images were observed at a set point current of 8 pA. The erasing of SC_1P–AuC typically occurred within 5–10 s.

convolution effect makes the lateral size larger than the expected planar dimension,[11] but accurate height information can be obtained. The mean tip height of the bright spots in the STM image (i.e., SC_1P–AuCs) was about 2.2 nm. This agrees with the SC_1P–AuC height of 2.2 nm, which is equal to the 1.0 nm core diameter plus two times the 0.6 nm size of SC_1P. Another important result was that most SC_1P–AuCs had similar heights, with a mean and standard deviation of 2.2 and 0.4 nm, respectively. This indicates that the SC_1P–AuCs have very similar structures even if different faces of the SC_1P–AuCs

dx.doi.org/10.1021/ja209634g | J. Am. Chem.Soc. 2012, 134, 816–819

attach to the substrate. Consequently, it is obvious that only a hexahedron satisfies these conditions among the possible structures that can be constructed from 6 ± 1 porphyrin faces.

Remarkably, the SC_1P–AuCs could be erased one by one by applying a sample bias voltage of 3 V (Figures 5a–d). It should be noted that the quality of the STM images for the SC_1P–AuCs did not degrade even after multiple erasing processes. The erasing mechanism is not clear but possibly includes multistep reductive dissociation or heat decomposition.[12] This phenomenon strongly supports that the structures observed on STM image are distinct SC_1P–AuCs. The STM images were observed even after the multiple erasing processes. This behavior of the SC_1P-AuCs could be applied to single cluster write-once read-many memory.

In this study, we developed a new strategy for introducing anisotropy to isotropic nanomaterials by constructing nano-Platonic solids. Nanohexahedra were successfully synthesized from six porphyrin derivatives around a Au cluster. These hexahedra are regarded as novel "artificial atoms" with anisotropically interactive faces. We believe that this approach using spherical nanoparticles is a novel self-assembly technique, because the formation of Platonic solid is automatically determined by the relationship between the diameter of the inscribed sphere and shapes/sizes of the polygonal faces. The present strategy could be expanded to other Platonic solids. Controlled fabrication of suprastructures from the clusters could be possible by assembling the nanohexahedra through coordination on the metal center of the metalloporphyrin derivatives. Furthermore, because of low tunnel resistance from the thin layer of protecting ligands and distance-dependent interaction between the porphyrin and Au cluster, the present hexahedra could function as Coulombic islands in single electron transistors. Research on single electron transistors using these hexahedra is now in progress.

■ ASSOCIATED CONTENT

Supporting Information

Synthesis of SC_nP, SC_nP–AuCs, SC_1, and SC_1-protected AuCs. Characterization of SC_1-protected AuCs. Sample preparation and instrumental setup for STM imaging. Single crystal X-ray crystallography of SC_nP. The complete list of authors for reference 2c. This material is available free of charge via the Internet at http://pubs.acs.org.

■ AUTHOR INFORMATION

Corresponding Author

teranisi@scl.kyoto-u.ac.jp

■ ACKNOWLEDGMENTS

The authors thank Prof. A. Sekiguchi and Dr. M. Ichinohe for their help with X-ray crystallography. The authors are grateful to the Chemical Analysis Center, University of Tsukuba, for elemental analysis data. This study was partially supported by a KAKENHI Grant-Aid for Scientific Research A (no. 23245028) (T.Teranishi) and a Grant-in-Aid for Scientific Research on Innovative Areas (grant no. 20108011, π-Space) from the Ministry of Education, Culture, Sports, Science and Technology (MEXT), Japan (Y.M.), by the Global COE Program of "Photonics Integration-Core Electronics" MEXT (Y.M.), by the Collaborative Research Project of Materials and Structures Laboratory, Tokyo Institute of Technology, and by the World Class University (WCU) Program through the Ministry of Education, Science and Technology of Korea (R31-10022) (Y.M.).

■ REFERENCES

(1) (a) Mann, S. *Nat. Mater.* **2009**, *8*, 781. (b) Glotzer, S. C.; Solomon, M. J. *Nat. Mater.* **2007**, *6*, 557. (c) Li, F.; Josephson, D. P.; Stein, A. *Angew. Chem., Int. Ed.* **2011**, *50*, 360. (d) Talapin, D. V.; Lee, J.-S.; Kovalenko, M. V.; Shevchenko, E. V. *Chem. Rev.* **2009**, *110*, 389.

(2) (a) Holst, J. R.; Trewin, A.; Cooper, A. I. *Nat. Chem.* **2010**, *2*, 915. (b) Mal, P.; Breiner, B.; Rissanen, K.; Nitschke, J. R. *Science* **2009**, *324*, 1697. (c) Tozawa, T.; et al. *Nat. Mater.* **2009**, *8*, 973. (d) Fujita, M.; Tominaga, M.; Hori, A; Therrien, B. *Acc. Chem. Res.* **2005**, *38*, 369.

(3) (a) Jones, M. R.; Macfarlane, R. J.; Lee, B.; Zhang, J.; Young, K. L.; Senesi, A. J.; Mirkin, C. A. *Nat. Mater.* **2010**, *9*, 913. (b) Park, S. Y.; Lytton-Jean, A. K. R.; Lee, B.; Weigand, S.; Schatz, G. C.; Mirkin, C. A. *Nature* **2008**, *451*, 553. (c) Doppelbauer, G.; Bianchi, E.; Kahl, G. *J. Phys.: Condens. Matter* **2010**, *22*, 104105. (d) Grzelczak, M.; Vermant, J.; Furst, E. M.; Liz-Marzán, L. M. *ACS Nano* **2010**, *4*, 3591. (e) Shirman, T.; Arad, T.; van der Boom, M. E. *Angew. Chem., Int. Ed.* **2010**, *49*, 926.

(4) DeVries, G. A.; Brunnbauer, M.; Hu, Y.; Jackson, A. M.; Long, B.; Neltner, B. T.; Uzun, O.; Wunsch, B. H.; Stellacci, F. *Science* **2007**, *315*, 358.

(5) Kanehara, M.; Takahashi, H.; Teranishi, T. *Angew. Chem., Int. Ed.* **2008**, *47*, 307.

(6) (a) Zhang, Y.-H.; Ruan, W.-J.; Li, Z.-Y.; Wu, Y.; Zheng, J.-Y. *Chem. Phys.* **2005**, *315*, 201. (b) Bose, K.; Huang, J.; Haggerty, B. S.; Rheingold, A. L.; Salm, R. J.; Walters, M. A. *Inorg. Chem.* **1997**, *36*, 4596.

(7) (a) Osuka, A.; Maruyama, K. *J. Am. Chem. Soc.* **1988**, *110*, 4454. (b) Muranaka, A.; Asano, Y.; Tsuda, A.; Osuka, A.; Kobayashi, N. *ChemPhysChem* **2006**, *7*, 1235.

(8) (a) Schaaff, T. G. *Anal. Chem.* **2004**, *76*, 6187. (b) Arnold, R. J.; Reilly, J. P. *J. Am. Chem. Soc.* **1998**, *120*, 1528.

(9) Tsunoyama, H.; Tsukuda, T. *J. Am. Chem. Soc.* **2009**, *131*, 18216.

(10) The sample preparation of SC_2P–AuCs was extremely difficult owing to their brittleness. Therefore, we could not observe the STM-image of SC_2P–AuCs.

(11) (a) Liljeroth, P.; Zeijlmans van Emmichoven, P. A.; Hickey, S. G.; Weller, H.; Grandidier, B.; Allan, G.; Vanmaekelbergh, D. *Phys. Rev. Lett.* **2005**, *95*, 086801. (b) Overgaag, K.; Vanmaekelbergh, D.; Liljeroth, P.; Mahieu, G.; Grandidier, B.; Delerue, C.; Allan, G. *J. Chem. Phys.* **2009**, *131*, 224510.

(12) (a) Widrig, C. A.; Chung, C.; Porter, M. D. *J. Electroanal. Chem.* **1991**, *310*, 335. (b) Azzaroni, O.; Vela, M. E.; Martin, H.; Hernández Creus, A.; Andreasen, G.; Salvarezza, R. C. *Langmuir* **2001**, *17*, 6647.

(13) Horcas, I.; Fernandez, R.; Gomez-Rodriguez, J. M.; Colchero, J.; Gómez-Herrero, J.; Baro, A. M. *Rev. Sci. Instrum.* **2007**, *78*, 013705.